International Journal on
"Technical and Physical Problems of Engineering"
(IJTPE)
Published by International Organization of IOTPE

ISSN 2077-3528
IJTPE Journal
www.iotpe.com
ijtpe@iotpe.com

March 2024 | Issue 58 | Volume 16 | Number 1 | Pages 73-79

DETERMINATION OF UNSTABLE AREA OPERATION OF DC/DC CONVERTER IN POWER SUPPLY SYSTEM OF AN AUTONOMOUS CONSUMER

I. Ivanov D. Kotin

Department of Electric Drive and Industry Automation, Novosibirsk State Technical University, Novosibirsk, Russia
i.a.ivanov@corp.nstu.ru, d.kotin@corp.nstu.ru

Abstract- This work is aimed at considering the area of instability in a microgrid system when the system is operated with a non-ideal energy source. This problem can occur in the power supply system of both autonomous consumers and in emergency power supply systems. In this study, a microgrid system with a DC bus with an active-inductive type of energy source is considered. A synchronous generator with permanent magnets acts as such a source, and a double active bridge acts as a semiconductor converter, in the form of simplified equivalent circuits. The system is considered in a quasi-steady process, which corresponds to its long-term operation, and also allows excluding from consideration the electromechanical processes occurring in the generator. To analyze the stability of the system, both the load parameters and the parameters of the transformation and the electrical parameters of the generator are used. The Rauss-Hurwitz method was used for stability analysis. As a result, using it, surfaces were obtained. The analysis of these surfaces made it possible to obtain groups of parameters that describe the boundaries of the stability of the system. An analysis of the obtained stability boundaries made it possible to establish the ratios of the system parameters at which the system is transferred to an unstable region. These results can be used in the synthesis of regulators of the voltage stabilizer control system to cut off the stable operation of the system.

Keywords: DC Microgrid, DC/DC Converter, Stability Analysis, Stability Boundary, CPL.

1. INTRODUCTION

Modern trends in the development of the energy industry associated with distributed generation and the use of green energy force the use of semiconductor converters in power supply systems for an autonomous consumer. This is due to the fact that the consumer must be the provision of high-quality electrical energy. At the moment, there is a wide variety of power supply systems for an autonomous consumer [1-4]. But the task of the considered power supply system's architectures is to ensure a reliable and stable power supply.

The types of architectures vary depending on the power consumption, but three types can be distinguished: AC system without intermediate bus, systems with intermediate DC bus, system with AC intermediate bus [2-4, 9]. Depending on the type of consumption, one or another system is selected. The most widely used system is with an intermediate DC bus, since this architecture requires synchronization only by voltage amplitudes and is necessary in the development of phase synchronization systems.

But as mentioned above, not only a reliable power supply is necessary, but also a stable one. The issue of stability in these systems can be considered from several angles. The problem of system stability becomes especially acute when the system is operating in an isolated mode and it is not possible to deal with it in any way due to external resources [4-10]. The first, when only the behavior of the consumer affects the system`s stability, and the second, when the stability of the system is influenced by all subsystems of the object. In this paper, the authors propose to consider the stability analysis of a microgrid autonomous object with a common intermediate DC bus, taking into account the type of energy source and the relationship between the parameters of the primary and secondary sides of a DC/DC converter with a load of the constant power load (CPL) type.

2. MATERIALS AND METHODS

To analyze the stable operation of the generating cell of a microgrid system with an intermediate DC bus, which includes equivalent circuits of a synchronous generator with a permanent magnet, presented as an EMF source with an active-inductive nature, a rectifier, DC/DC converter with input and output filters, we set a typical block diagram shown in Figure 1 [11-13].

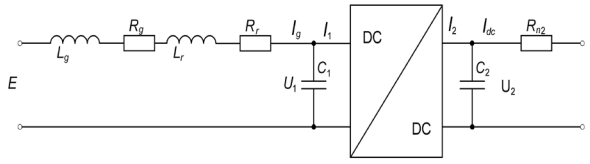

Figure 1. Energy supply system [11]

Registered: 230722 | Article Info: 1701 | Accepted: 240224
Reserved: 240119 | Available: 240331

The system consists of PMSM, rectifier, Bidirectional H-Bridge DC/DC converter input filter, output filter, CPL, which the mathematical description contains the structure [11]:

$$\begin{cases} E=(R_g+R_r)I_g+(L_g+L_r)pI_g+U_1= \\ =R_1I_g+L_1pI_g+U_1 \\ U_1=\dfrac{1}{C_1p}(I_g-I_1) \\ \rightarrow I_g=C_1pU_1+I_1 \\ U_1=\dfrac{U_1^2}{-P_n}I_1=-R_{n1}I_1 \\ \dfrac{I_1}{I_2}=K \\ U_2=\dfrac{1}{C_2p}(I_2-I_{dc}) \\ \rightarrow I_2=C_1pU_2+I_{dc} \\ U_2=\dfrac{U_2^2}{-P_n}I_{dc}=-R_{n2}I_{dc} \end{cases} \quad (1)$$

where, E is the EMF, and R_g, R_r, R_1 are the active component of the resistances of the genera-tor, rectifier and the active resistance of the primary side of the DC/DC converter, L_g, L_r, L_1 is the inductive component of the resistances of the generator, rectifiers and the impedance inductive resistance of the primary side of the DC/DC converter, I_g is generator current, U_1, U_2 are voltage on the primary and secondary side of the DC/DC converter, I_1, I_2 are current in the primary and secondary part of the DC/DC converter, C_1, C_2 are capacitance of the input and output filters of the DC/DC converter, and P_n of CPL, R_{n1}, R_{n2} are active component of the load resistance driven to the primary and secondary side of the DC/DC converter

To simplify the analysis, namely the influence of the load on the stability of the system, we bring the parameters of the secondary side to the primary side [11]:

$$\frac{U_2}{U_1}=K \quad (2)$$

$$\rightarrow U_2=KU_1$$

$$R_{n2}=\frac{U_2^2}{P_n}=\frac{(KU_1)^2}{P_n}=K^2\frac{U_1^2}{P_n}=K^2R_{n1} \quad (3)$$

$$C_2=aC_1 \quad (4)$$

where, a is a coefficient describing the ratio of input and output DC/DC converter.

For analysis from system (1) and taking into account the accepted parameters (2)-(4), a small signal model in (5) [11]:

$$p\begin{bmatrix} i_{\Delta g} \\ i_{\Delta 1} \\ i_{\Delta 2} \end{bmatrix}=\begin{bmatrix} -\dfrac{R_1}{L_1} & \dfrac{R_{n1}}{L_1} & 0 \\ -\dfrac{1}{C_1R_{n1}} & \dfrac{1}{C_1R_{n1}} & 0 \\ 0 & \dfrac{1}{K^3aC_1R_{n1}} & -\dfrac{1}{K^2aC_1R_{n1}} \end{bmatrix}\times \quad (5)$$

$$\times\begin{bmatrix} i_{\Delta g} \\ i_{\Delta 1} \\ i_{\Delta 2} \end{bmatrix}+\begin{bmatrix} \dfrac{1}{L_1} \\ 0 \\ 0 \end{bmatrix}\times\begin{bmatrix} E_\Delta \\ 0 \\ 0 \end{bmatrix}$$

General transfer function [11]:

$$W_g(s)=\frac{i_{\Delta dc}(s)}{E_\Delta(s)}=\frac{1}{T_3s^3+T_2s^2+T_1s+1} \quad (6)$$

where,

$$T_3=-aL_1C_1^2K^3R_{n1}^2 \quad (7)$$

$$T_2=aK^3C_1R_{n1}L_1-aK^3C_1^2R_1R_{n1}^2-KL_1C_1R_{n1} \quad (8)$$

$$T_1=KL_1-KC_1R_1R_{n1}+aK^3R_1C_1R_{n1}-aK^3C_1R_{n1}^2 \quad (9)$$

$$T_0=K(R_1-R_{n1}) \quad (10)$$

To determine the stable performance of the system, a general transfer function of the entire system is characteristic (6). For further analysis, we compose the equation of the first determinant a_0 of the Routh-Hurwitz matrix [11]:

$$a_0=T_2T_1-T_0T_3=f(a,K,R_{n1}) \quad (11)$$

where,

$$\begin{aligned} &f(a,K,R_n1)=C_1^2R_1(a^2K^6R_{n1}^4)+C_1^3R_1^2(aK^4R_{n1}^3)- \\ &-C_1^3R_1^2(a^2K^6R_{n1}^3)-C_1^2L_1(a^2K^6R_{n1}^3)+ \\ &+C_1^2(a^2K^4R_{n1}^3)-C_1^2L_1(aK^4R_{n1}^3)+C_1L_1^2(aK^4R_{n1}^2)- \\ &-C_1^2L_1R_1(aK^4R_{n1}^2)-C_1^2L_1R_1(aK^4R_{n1}^2)+ \\ &+C_1^2L_1R_1(K^2R_{n1}^2)+C_1^2L_1R_1(aK^6R_{n1}^2)- \\ &-C_1^2L_1R_1(aK^4R_{n1}^2)+C_1^2L_1R_1(aK^4R_{n1}^2)- \\ &-C_1L_1^2(K^2R_{n1}) \end{aligned} \quad (12)$$

Since the analysis and construction of a four-dimensional space is difficult, we will analyze its three-dimensional projections on each of the axes. Also, to simplify the analysis of three-dimensional figures, which are projections of a four-dimensional space, we will divide them into a set of surfaces. Thus, we can say that in order to evaluate the nature of a four-dimensional spacer`s behavior. It will be necessary to project it onto three three-dimensional spaces, and then the resulting three-dimensional figures, which will be divided into the n-th number of surfaces [11]:

$$a_0=f(a,K,R_{n1})=\begin{cases} a_0=f(K(a),R_{n1}(a)), \\ a_0=f(a(K),R_{n1}(K)), \\ a_0=f(a(R_{n1}),K(R_{n1})). \end{cases} \quad (13)$$

To determine the exact boundary of the stability of the system, it was solved to find the curves describing the intersections of the surfaces of zeros with the corresponding surfaces [11]:

$$a_0 = f\left(a, K, R_{n1}\right) = 0 = \begin{cases} a_0 = f_{a=\text{var}}\left(K\right) = 0 \\ a_0 = f_{a=\text{var}}\left(R_{n1}\right) = 0 \\ a_0 = f_{K=\text{var}}\left(a\right) = 0 \\ a_0 = f_{K=\text{var}}\left(R_{n1}\right) = 0 \\ a_0 = f_{R_{n1}=\text{var}}\left(a\right) = 0 \\ a_0 = f_{R_{n1}=\text{var}}\left(K\right) = 0 \end{cases} \quad (14)$$

i.e., we obtain a curve describing the intersection of two surfaces for different values of the constant coefficient with the zero plane. To determine the functions of these surfaces, we interpolate in the boundary`s region of the surfaces intersection of the systems.

3. RESULTS

To implement this, we will set a discrete step for changing the constant parameters and variable parameters of the function. In the first case, the change in the coefficient of dependence of the output capacitance on the input a, a constant parameter. It will be in the range from 1 to 10 with a step of 1, and the variable coefficients of the function, transformation ratio K from 0.5 to 3. The equivalent active resistance of the power consumption R_{n1} in the range of recalculation of the power consumption from 1 kW to 75 kW. In the second case, the change in the transformation ratio K, a constant parameter. It will be in the range from 0.5 to 3 in increments of 0.5, and the variable coefficients of the function, the coefficient of dependence of the output capacitance on the input a from 1 to 10. The equivalent active resistance of the consumed power R_{n1} in the range of recalculation of power consumption from 1 kW to 75 kW.

In the third case, the change in the equivalent active resistance of the power consumption R_{n1}, a constant parameter. It will be in the CPL range from 1 kW to 75 kW in increments of 5 kW, and the variable coefficients of the function. The dependence coefficient of the output capacitance on the input a from 1 to 10, and the transformation ratio K is from 0.5 to 3.

Figures 2-7 show the surfaces for two extreme values of the constant parameter when using the system of Equations (12) and (13).

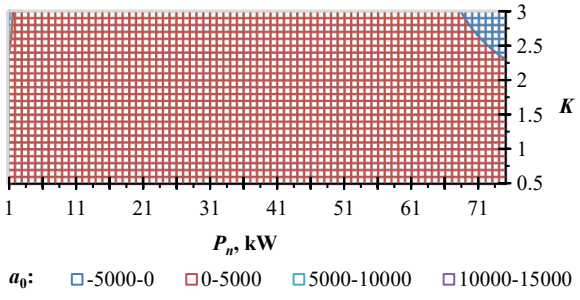

Figure 2. Surface $a_0 = f(K, P_n)$, for $a = 1$ [11]

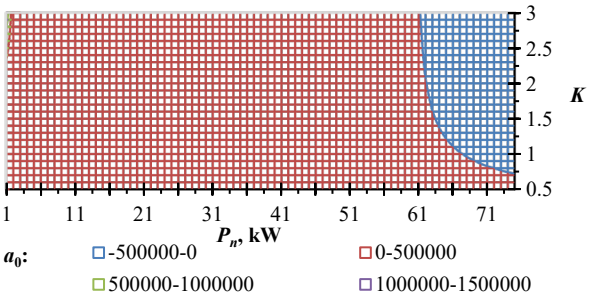

Figure 3. Surface $a_0 = f(K, P_n)$, for $a = 10$ [11]

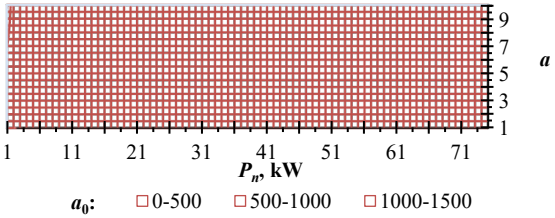

Figure 4. Surface $a_0 = f(a, P_n)$, for $K = 0.5$ [11]

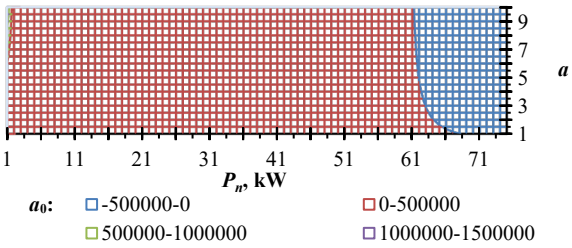

Figure 5. Surface $a_0 = f(a, P_n)$, for $K = 3$ [11]

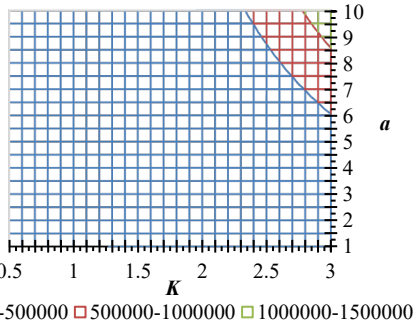

Figure 6. Surface $a_0 = f(a, K)$, for $P_n = 1$ kW [11]

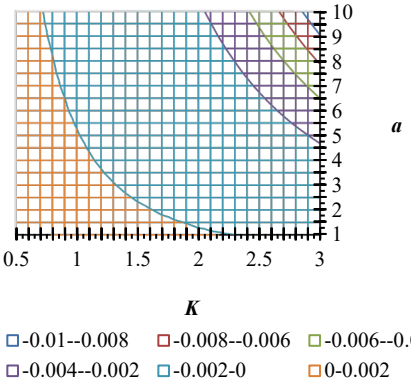

Figure 7. Surface $a_0 = f(a, K)$, for $P_n = 75$ kW [11]

In all three sets of surfaces, a system instability zone appears, and when any constant surface parameter changes, this zone changes, namely, the system instability zone increases.

When considering the proportional capacitance coefficient as a constant parameter of the system, it can be seen that the instability zone of the system occurs at its minimum value, as shown in Figure 2. With an increase in the coefficient, a nonlinear the area expansion of zone occurs both in terms of the parameter transfer coefficient and in terms of power consumption, as shown in Figure 3. Comparing the zones of instability with a minimum conception of the proportional capacitance coefficient, the instability zone expands by about 8 times. In this case, the maximum allowable trans-mission coefficient at which the system is stable at maximum power decreases from 2.3 to 0.7. The value of the transmitted power at the maximum transmission coefficient decreases from 68 to 61 kW [11].

If we take the transmission coefficient of the converter as a constant parameter, then a similar effect is observed. At the minimum value of the transmission coefficient, the system does not have a zone of instability, as shown in Figure 4. Its increase leads to the appearance of this zone, as shown in Figure 5. In the previous case, a non-linear expansion of the instability zone occurs, as shown in Figure 5. The instability zone occurs at a transfer coefficient of 1. When the coefficient is increased to 3, the capacitance proportional maximum coefficient increases from 5 to 0, i.e., with a trans-formation ratio of 3, the system cannot be stable at a maximum power consumption of 75 kW, so the coordinate of the maximum is shifted to a point to 68 kW. The maximum transmitted power at the maximum capacitance ratio changes from 67 to 61 kW [11].

When considering the power consumption as a constant coefficient, it is clear that with a minimum power consumption, the system is stable in its entire range of parameters, as shown in Figure 6. In the first, the instability zone appears at 60 kW and begins to rapidly increase in size until reaching 75 kW. With the maximum capacitance ratio, the transfer ratio of the pre-distorter changes from 1.2 to 0.8, and at the maximum transfer coefficient, the value of the capacitance proportionality coefficient changes from 1.5 to 0. In order to ensure the minimum value of the transfer coefficient at which the system can be stable, it is necessary to reduce the transfer coefficient to 2.7 [11].

After constructing the surfaces and obtaining the intersection curve of the surfaces, the curves were obtained. These curves describe the stability boundary of the system for different values of the coefficients of proportionality of the output capacitance of the input capacitance when the load and transmission coefficient change, a set of curves is shown in Figures 8-13.

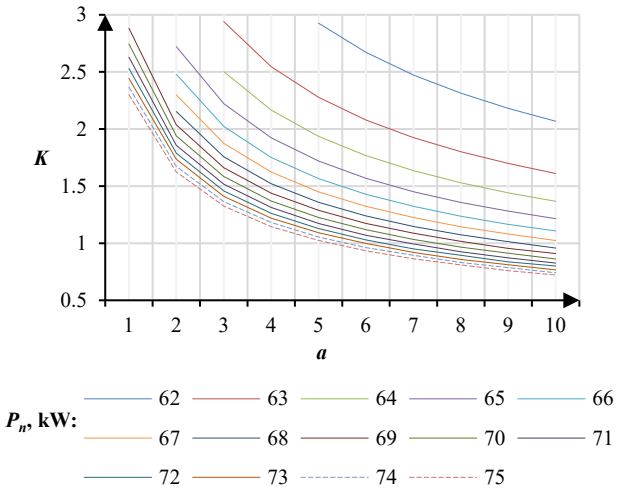

Figure 8. Stability limit's function $a_0 = f_{a=\text{var}}(K)$ for $P_n = \text{const}$ [11]

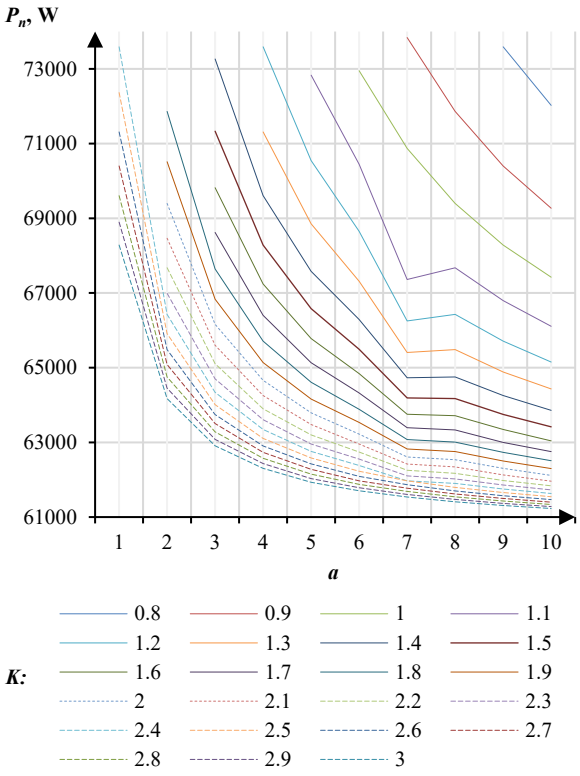

Figure 9. Stability limit's function $a_0 = f_{a=\text{var}}(P)$ for $K = \text{const}$ [11]

Analyze Figures 8-7 to determine the patterns of behavior of the system's stability boundary. The figures describing the behavior of the resistance stability boundary under the condition $P = \text{const}$, the functions on Figures 8 and 10, it can be seen that with an increase in the power consumption, the instability boundary expands both in terms of the gain parameter and in terms of the capacitance proportionality factor. The same behavior of the stability boundary can be traced under the condition $a = \text{const}$, functions on Figure 11 and Figure 6, and under the condition $K = \text{const}$, the functions on Figures 9 and 7.

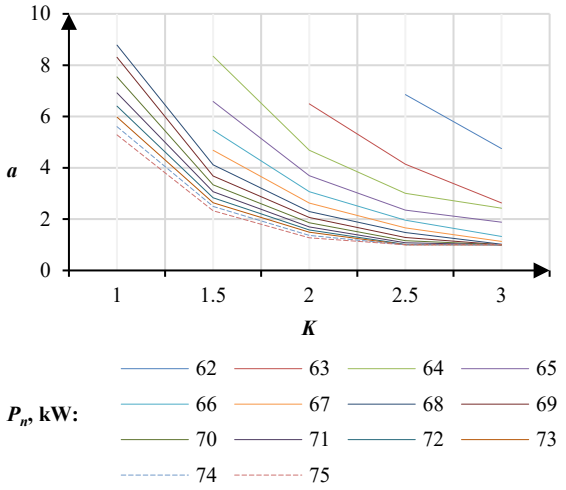

Figure 10. Stability limit's function $a_0 = f_{K=\text{var}}(a)$ for $P_n = \text{const}$ [11]

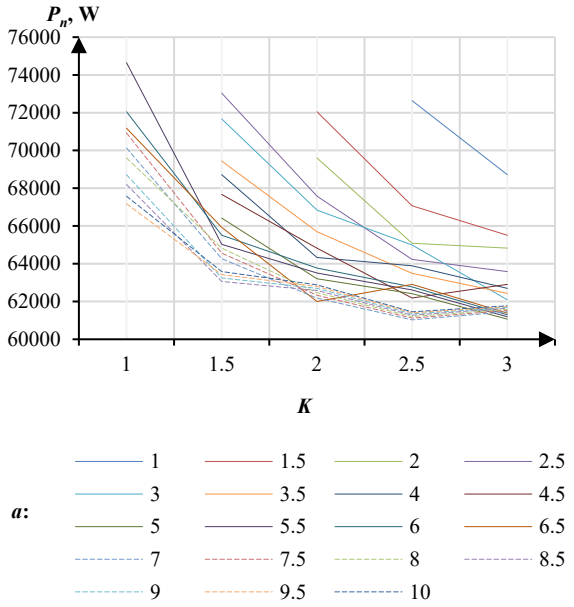

Figure 11. Stability limit`s function $a_0 = f_{K=\text{var}}(P)$ for $a = \text{const}$ [11]

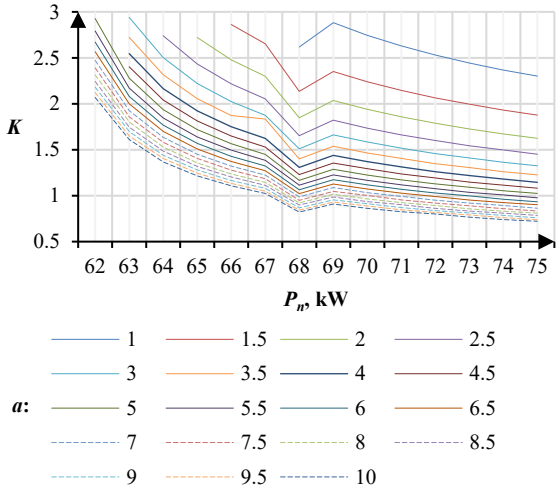

Figure 12. Stability limit's function $a_0 = f_{P=\text{var}}(K)$ for $a = \text{const}$ [11]

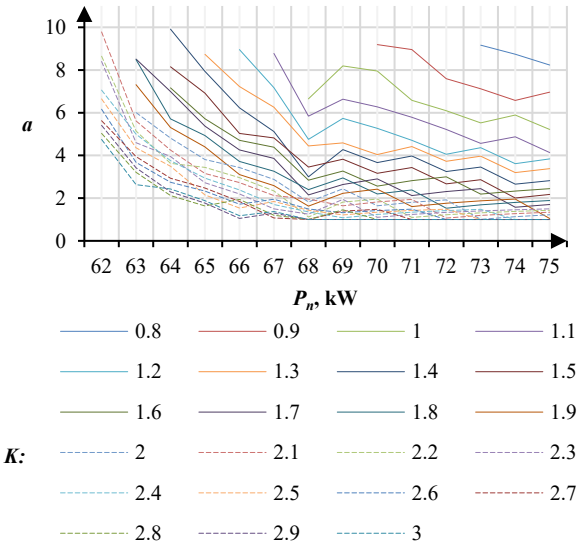

Figure 13. Stability limit's function $a_0 = f_{P=\text{var}}(a)$ for $K = \text{const}$ [11]

The results obtained demonstrate that an instability zone appears in the DC/DC converter system. The region of the instability zone is affected by three indicators that connect the primary and secondary sides of the DC/DC converters. Since, as a result of the analysis, 6 sets of curves were obtained that describe the movement of the stability boundary, it is necessary to determine the most convenient class of curves for synthesis of control system.

According to the authors, the most convenient for the synthesis of the control system will be the curves given by the condition $a = \text{const}$, such sets of curves are the functions on Figure 11 and Figure 12. Use as the reference parameter of the coefficient a is explained by the fact that this coefficient has a constant value and is set at the stage of system development. From Figure 11 it can be seen that from the coefficient of proportionality of the capacitance in system, distortions arise in monotonicity of decrease in the functions of the stability boundaries of the system.

At $a = 4.5$, an extremum appears in the system at a value of $K = 2.5$. At $a = 6.5$, two inflections of the function appear in the system at $K = 2$ and $K = 2.5$. And within the boundaries a from 7 to 10, an extremum is observed in the system at the point $K = 2.5$. Figure 12 shows that the class of functions has an identical form of monotonicity over its entire range of definition. A point stands out from the general form of monotony at a power of 68 kW. At this point, there is a local minimum of the function, and at the point of 69 kW there is an inflection point for all functions. Moreover, it should be noted that with an increase in the coefficient, a, there is a decrease in the value of the maximum deviation of the gain at the point of 68 kW, relative to the general nature of the decrease in the function.

As can be seen from the behavior`s description of the functions class of the system`s stability boundary, the simplest in terms of the formation of a generalized mathematical function of the upper boundary of the

power factor is the curves class shown in Figure 12. Based on this description, it is possible to develop a nonlinear controller of the form $K = f(K)$, for known fixed a. This controller will limit the energy transfer coefficient K between the primary and secondary side of the DC/DC converter to ensure a stable mode of operation of the system.

6. DISCUSSION

The results obtained demonstrate that an instability zone appears in the DC/DC converter system. The region of the instability zone is affected by three indicators that connect the primary and secondary sides of the DC/DC converters. Since, as a result of the analysis, six sets of curves were obtained that describe the movement of the stability boundary, it is necessary to determine the most convenient class of curves for the synthesis of the control system. According to the authors, the most convenient for the synthesis of the control system are the curves given by the condition $a = \text{const}$; such sets of curves are the functions $a_0 = f_{K=\text{var}}(P)$, as shown in Figure12, and $a_0 = f_{P=\text{var}}(K)$, as shown in Figure13. The reference parameter of the coefficient a is explained by the fact that this coefficient has a constant value and is set at the stage of system development. From Figure 12 it can be seen that from the coefficient of proportionality of the capacitance in the system, distortions arise in the monotonicity of the decrease in the functions of the stability boundaries of the system. At $a = 4.5$, an extremum appears in the system at a value of $K = 2.5$. At $a = 6.5$, two inflections of the function appear in the system at $K = 2$ and $K = 2.5$. Within the boundaries of a from 7 to 10, an extremum is observed in the system at the point $K = 2.5$. Figure 13 shows that the class of functions has an identical form of monotonicity over its entire range of definition. A point stands out from the general form of monotony at a power of 68 kW. At this point, there is a local minimum of the function, and at the point of 69 kW there is an inflection point for all functions. Moreover, it should be noted that with an increase in the coefficient, a, there is a decrease in the value of the maximum deviation of the gain at point of 68 kW, relative to general nature of decrease in the function.

As can be seen from the behavior`s description of the functions class of the system`s stability boundary, the simplest in formation generalized mathematical function terms of a of the upper boundary of the power factor is the class of curves shown in Figure 13. Based on this description, it is possible to develop a nonlinear controller of the function of the form $K = f(K)$, for known fixed a. This controller limits the energy transfer coefficient K between the primary and secondary side of the DC/DC converter to ensure a stable mode of operation of system.

The study of the influence of this additional controller on the control system will be carried out in the next work of the team of authors. An analysis of the structure of the control system with its use will also be carried out. This will make it possible to perform structural optimization of the system control algorithm.

7. CONCLUSIONS

As a result of this work, it was found that an instability region can occur in a microgrid system, taking into account the nature of the behavior of the energy source and the internal parameters of the semiconductor converter. The influence on the given region of instability of the system of the power of the consumer, the transmission coefficient and the coefficient of the ratio of the capacitance values of the filters of the lower and upper sides was analyzed. As a result of this analysis, stability boundaries were obtained, which depend on two of the above parameters with a constant value of the third. From the analysis of the behavior of the stability boundary curves, it was established that the system instability boundary is in the upper boundaries of two variable parameters, but when the value of the third parameter remains unchanged, it increases and tends to the values of the lower boundaries of the variable parameters. These results demonstrate the emergence of an instability zone in the microgrid system, which depends not only on the power and behavior of the consumer, but also on the parameters of the converter itself and the parameters and behavior of the energy source. The use of these results is possible in the synthesis of the voltage stabilizer control system. The implementation of these results and the study of success of their application will be a topic for further study.

NOMENCLATURES

1. Acronyms

DC	Direct Current
AC	Alternating Current
CPL	Constant Power Load
EMF	Electromotive Force

2. Symbols / Parameters

E : The EMF

R_g : The active resistances of the generator

R_r : The active resistances of the rectifier

R_1 : The active of the primary side

L_g : The inductive resistances of the generator

L_r : The inductive resistances of the rectifier

L_1 : The inductive resistances of the primary side

I_g : The generator current

U_1 : The voltage on the primary side

U_2 : The voltage on the secondary side

I_1 : The current in the primary part

I_2 : The current in the secondary part

I_{dc} : The load current`s

C_1 : The capacitance of the input filters

C_2 : The capacitance of the output filters

P_n : The CPL

R_{n1} : The active component of the load resistance on to the primary side

R_{n2} : The active component of the load resistance on to the secondary side
a : The coefficient describing the ratio of input and output filter capacitance
p : The differential operator
T_3 : The time constant transfer function
T_2 : The time constant transfer function
T_1 : The time constant transfer function
a_0 : The first determinant of the Routh-Hurwitz matrix

REFERENCES

[1] D.E. Olivares, et al., "Trends in Microgrid Control", IEEE Trans Smart Grid, Vol. 5, No. 4, pp. 1905-1919, 2014.
[2] A. El Shahat, S. Sumaiya, "DC-Microgrid System Design, Control, and Analysis", Electronics, Vol. 8, No. 2, p. 124, January 2019.
[3] M. Rezkallah, A. Chandra, B. Singh, S. Singh, "Microgrid: Configurations, Control and Applications", IEEE Trans Smart Grid, Vol. 10, No. 2, pp. 1290-1302, March 2019.
[4] E. Yusubov, L.R. Bekirova "A Robust Metaheuristic Central Controller for Hierarchical Control System with Adaptive Power Sharing and MPPT in DC Microgrids", International Journal on Technical and Physical Problems of Engineering (IJTPE), Issue 53, Vol. 14, No. 4, pp. 392-399, December 2022.
[5] I. Khan, Y. Xu, H. Sun, V. Bhattacharjee, "Distributed Optimal Reactive Power Control of Power Systems", IEEE Access, Vol. 6, pp. 7100-7111, December 2017.
[6] C. Wan, M. Huang, C.K. Tse, X. Ruan, "Stability of Interacting Grid-Connected Power Converters", Journal of Modern Power Systems and Clean Energy, Vol. 1, No. 3, pp. 249-257, January 2013.
[7] Y. Gui, F. Blaabjerg, X. Wang, J.D. Bendtsen, D. Yang, J. Stoustrup, "Improved DC-Link Voltage Regulation Strategy for Grid-Connected Converters", IEEE Transactions on Industrial Electronics, Vol. 68, No. 6, pp. 4977-4987, June 2021.
[8] Y.V. Pavan Kumar, R. Bhimasingu, "Renewable Energy Based Microgrid System Sizing and Energy Management for Green Buildings", Journal of Modern Power Systems and Clean Energy, Vol. 3, No. 1, pp. 1-13, January 2015.
[9] S.N. Tackie, "A Review of Control Techniques in AC/DC and Hybrid Microgrid", International Journal on Technical and Physical Problems of Engineering (IJTPE), Issue 55, Vol. 15, No. 2, pp. 6-13, June 2023.
[10] P.O. Kriett, M. Salani, "Optimal Control of a Residential Microgrid", Energy, Vol. 42, No. 1, pp. 321-330, June 2012.
[11] D. Kotin, I. Ivanov, "The Stable Operation Analysis of the DC Converter System into a Microgrid System, Taking into Account the Parameters of the Energy Source and the Own Parameters of the DC Converter", preprints.org, 2022120173, Version 1, December 2022.
[12] A.M. Hashimov, N.R. Rahmanov, N.M. Tabatabaei, H.B. Guliyev, F.Sh. Ibrahimov, "Probabilistic evaluation of voltage stability limit of power system under the conditions of accidental Emergency outages of lines and generators", International Journal on "Technical and Physical Problems of Engineering" (IJTPE), Vol. 12, No. 2, pp. 40-45, June 2020
[13] N. Genc, "PV based *v/f* controlled induction motor drive for water pumping", International Journal on "Technical and Physical Problems of Engineering" (IJTPE), Vol. 12, No. 4, pp. 103-108, December 2020

BIOGRAPHIES

Name: **Ilya**
Surname: **Ivanov**
Birthday: 08.11.1995
Birthplace: Barnaul, Russia
Bachelor: Automatization and Electric Drive, Department, Power Engineering Faculty, Polzunov Altay State Technical University, Barnaul, Russia, 2018
Master: Synthesis of Automatic Control Systems for Electric Drives, Department, Power Engineering Faculty, Polzunov Altay State Technical University, Barnaul, Russia, 2020
Doctorate: Student, Electrical Complexes and Systems, Department of Electric Drive and Industry Automation, Faculty Mechatronics and Automation, Novosibirsk State Technical University, Novosibirsk, Russia, Since 2020
Research Interests: Control System, Power Converter
Scientific Publications: 7 Papers, 2 Books, 28 Patents, 2 Projects, 54 Theses

Name: **Denis**
Surname: **Kotin**
Birthday: 30.05.1984
Birthplace: Novosibirsk, Russia
Bachelor: Control Systems of Electric Drives, Department of Electric Drive and Industry Automation, Faculty of Mechatronics and Automation, Novosibirsk State Technical University, Novosibirsk, Russia, 2005
Master: Control Systems of Electric Drives, Department of Electric Drive and Industry Automation, Faculty of Mechatronics and Automation, Novosibirsk State Technical University, Novosibirsk, Russia, 2007
Doctorate: Electrotechnical Complexes and Systems, Department of Electric Drive and Industry Automation, Faculty Mechatronics and Automation, Novosibirsk State Technical University, Novosibirsk, Russia, 2010
The Last Scientific Position: Assoc. Prof., Department of Electric Drive and Industry Automation, Faculty Mechatronics and Automation, Novosibirsk State Technical University, Novosibirsk, Russia, Since 2010
Research Interests: Control System, Power Converter
Scientific Publications: 45 Papers, 8 Books, 10 Patents, 2 Projects, 75 Theses